Simultaneous Control of Flexibility and Rigidity in Pore-Space-Partitioned Metal-Organic Frameworks

Yuchen Xiao,[a] Yichong Chen,[a] Wei Wang,[a] Huajun Yang,[b] Anh N. Hong,[a] Xianhui Bu,*[,b] Pingyun Feng,*[,a]

[a] Department of Chemistry, University of California, Riverside, California 92521, United States

[b] Department of Chemistry and Biochemistry, California State University, Long Beach, California 90840, United States

KEYWORDS: pore space partition, flexible MOF, bioisosteric, ultrasmall pore, gas separation

ABSTRACT: Flexi-MOFs are typically limited to low-connected (< 9) frameworks. Here we report a platform-wide approach capable of creating a family of high-connected materials (collectively called CPM-220) that integrate exceptional framework flexibility with high rigidity. We show that the multi-module nature of the pore-space-partitioned *pacs* (partitioned *acs* net) platform allows us to introduce flexibility as well as to simultaneously impose high rigidity in a tunable module-specific fashion. The inter-modular synergy has remarkable macro-morphological and sub-nanometer structural impacts. A prominent manifestation at both length scales is the retention of X-ray-quality single crystallinity despite huge hexagonal *c*-axial contraction (≈ 30%) and harsh sample treatment such as degassing and sorption cycles. CPM-220 sets multiple precedents and benchmarks on the *pacs* platform in both structural and sorption properties. They possess exceptionally high benzene/cyclohexane selectivity, unusual C_3H_6 and C_3H_8 isotherms, and promising separation performance for small gas molecules such as C_2H_2/CO_2.

Storage and separation of gas or vapor molecules benefit from enhanced host-guest interactions resulting from small and ultrasmall pore size that is commensurate with size of adsorbate molecules.[1-9] However, pore control in small-pore regime is constrained by limited availability of building blocks, in part because small molecular building units offer less room and sites for chemical editing. Recently, pore space partition (**PSP**) which uses a complementary ligand to segment pore space was introduced.[10-11] A representative example of PSP is the *pacs* prototype (***pacs*** = partitioned *acs*), a multi-modular system formulated as $[(M1)_x(M2)_{3-x}(O/OH)(L1)_3(L2)]$.[12-25] In *pacs*, the *acs*-type (MIL-88/MOF-235) framework formed by metal trimers and ditopic L1 ligand is partitioned by pore-partitioning L2 ligand into small pockets.

While PSP is suited for engineering both large- and small-pore structures by using L1 and L2 ligands of various dimensions, it has unique advantages for designing small-pore architecture. To push down the boundary of pore-size, we recently applied the integrative **BIS-PSP** strategy to the MOF synthesis.[22-23] This strategy is the combined use of PSP with the bioisosteric (**BIS**) concept (i.e., mimicking aromatic entity with aliphatic one), which has led to the synthesis of *pacs* materials from rigid and 3D sp^3-C-based bcp ligand. Among reported *pacs* materials, bcp is the shortest L1 ligand,[22] and notably it has only 3 atoms between COO^- groups (based on the path shown in red, **Scheme 1**), compared to 4 in bdc,[13] cdc,[22] and bco,[23] 6 in 2,6-ndc,[13] and 8 in bpdc.[13]

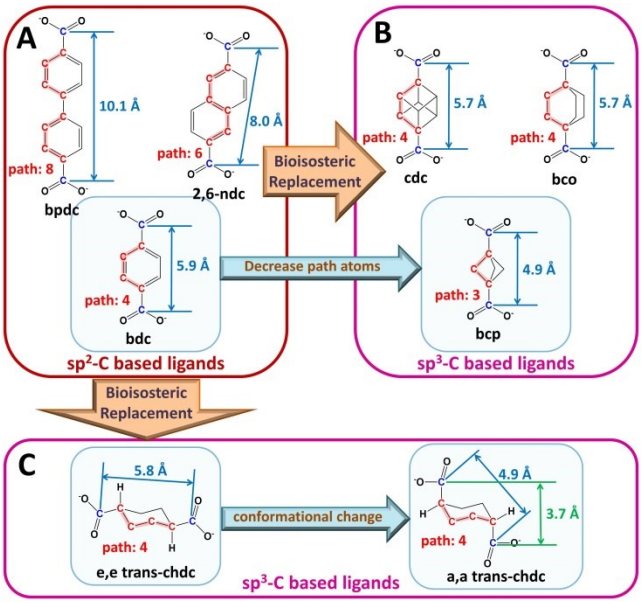

Scheme 1. The evolution as well as paradigm shift for L1 ligand design on *pacs* platform. (A→B) rigid sp^2-to-sp^3 BIS strategy with concurrent control of path length and core structure; (A→C) sp^2-to-sp^3 flexi-BIS strategy. (A, B, C) in this work, the conformational change (ring flipping) enables an extra level of pore control with an effect greater than that produced by ring shortening to bcp. bcp = bicyclo[1.1.1]pentane-1,3-dicarboxylate, bdc = benzene-1,4-dicarboxylate, cdc = cubane-1,4-dicarboxylate, bco = bicyclo[2.2.2]octane-1,4-dicarboxylate, 2,6-ndc = naphthalene-2,6-dicarboxylate, bpdc = biphenyl-4,4'-dicarboxylate.

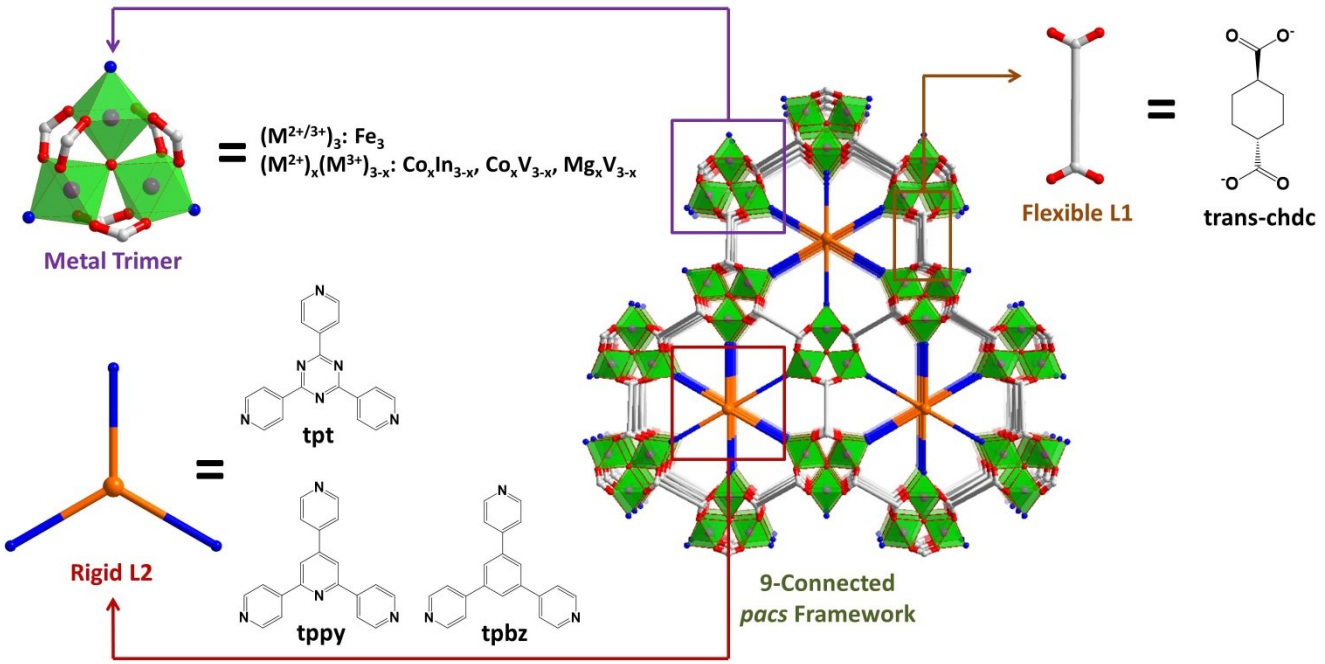

Figure 1. Illustration of tri-modules of the first flexi-rigid *pacs* system. tpt = 2,4,6-tri(4-pyridyl)-1,3,5-triazine), tppy = 2,4,6-tris(4-pyridyl)pyridine, tpbz = 1,3,5-tri(4-pyridyl)benzene.

Given the limited availability of small building blocks, especially the rigid type, we envision an alternative path forward by extending the BIS-PSP strategy to flexible aliphatic L1 ligand types for the first time on the *pacs* platform. This strategy (**flexi-BIS-PSP**) would permit the creation of a multi-modular 9-connected *pacs* platform (**flexi-*pacs***) that integrates flexi-L1 ligands with rigid L2 ligands. Note that lattice-flexible MOFs are generally low-connected (< 9).[26-36] We show here that the PSP concept offers a platform-wide and modular-based approach to create flexibility in high-connected frameworks in which flexibility and rigidity are subject to individual modular control. Moreover, the inter-modular synergy on the *pacs* platform can enable the use of more L1 ligand types, leading to a much larger isoreticular family.[37-40]

Since its inception, PSP has been known and used for its ability to rigidify the framework. For example, the PSP strategy, which converts 6-connecetd *acs* net into 9-connected *pacs* net, easily freezes swelling effect in MIL-88. Here, with flexi-BIS-PSP, the return of framework flexibility through L1 ligand and its interplay with rigidifying effect of PSP represents a unique phenomenon and paradigm shift. The multi-module nature of the *pacs* platform makes it possible to bestow framework flexibility with one module while at the same time to add framework rigidity with another module. Additionally, the inter-modular synergy helps prevent a well-known pitfall in flexi-MOFs (i.e., the formation of closed phases).

Here, we report a family of *pacs*-MOFs (CPM-220) based on trans-1,4-cyclohexanedicarboxylate (**chdc**, L1).[41-45] The conformational flexibility from L1 ligand and the rigidity from L2 ligand (the PSP effect) lead to exceptional flexibility in the hexagonal *c* direction and yet high rigidity in basal directions (*a*/*b*). Remarkably, CPM-220 retains its single crystallinity (single-crystal to single-crystal transformation) throughout solvent exchange, degassing, and gas sorption cycles despite a huge percentage change in the *c* axis length and cell volume (≈ 30%). CPM-220 has unusual sorption properties for C_3H_6 and C_3H_8, excellent benzene/cyclohexane selectivity, and promising properties for separating small gas molecules (e.g., C_2H_2/CO_2).

Due to its multi-module nature and superior ability to accommodate different trimer- and L2-types, CPM-220 can be made in many compositions by varying trimer or L2 modules. Here we report six compositions from four trimer types and three L2 types (**Figure 1**, **Table S3**). For each composition, the as-synthesized form with the longest *c* axis is denoted **phase 1**, and the degassed form with the shortest *c* axis is denoted **phase 2**. Both single-crystal X-ray diffraction (SCXRD) and powder X-ray diffraction (PXRD) show that phase 1 undergoes a gradual change to phase 2 under ambient conditions. **Table S4A** summarizes unit cell parameters and *c*/*a* ratios.

For **CoIn-chdc-tpt**, from phase 1 to phase 2, the *a*/*b* axis is almost unchanged (16.95 to 17.08 Å), but the *c* axis is shortened by 4.76 Å (or 31.32%) from 15.20 to 10.44 Å. Correspondingly, the cell volume is reduced by 30.19% from 3779 to 2638 Å^3. The similar change occurs for CoV-chdc-tpt. The *c* axis of 10.44 Å and the *c*/*a* ratio of 0.61 are both the smallest values so far on the *pacs* platform (**Figure 2**) and are significantly lower than 12.1 Å and 0.71 in bcp *pacs*.[22] The cell parameters and *c*/*a* ratios are closely watched values on the *pacs* platform because they have direct correlation with pore dimensions and sorption properties.

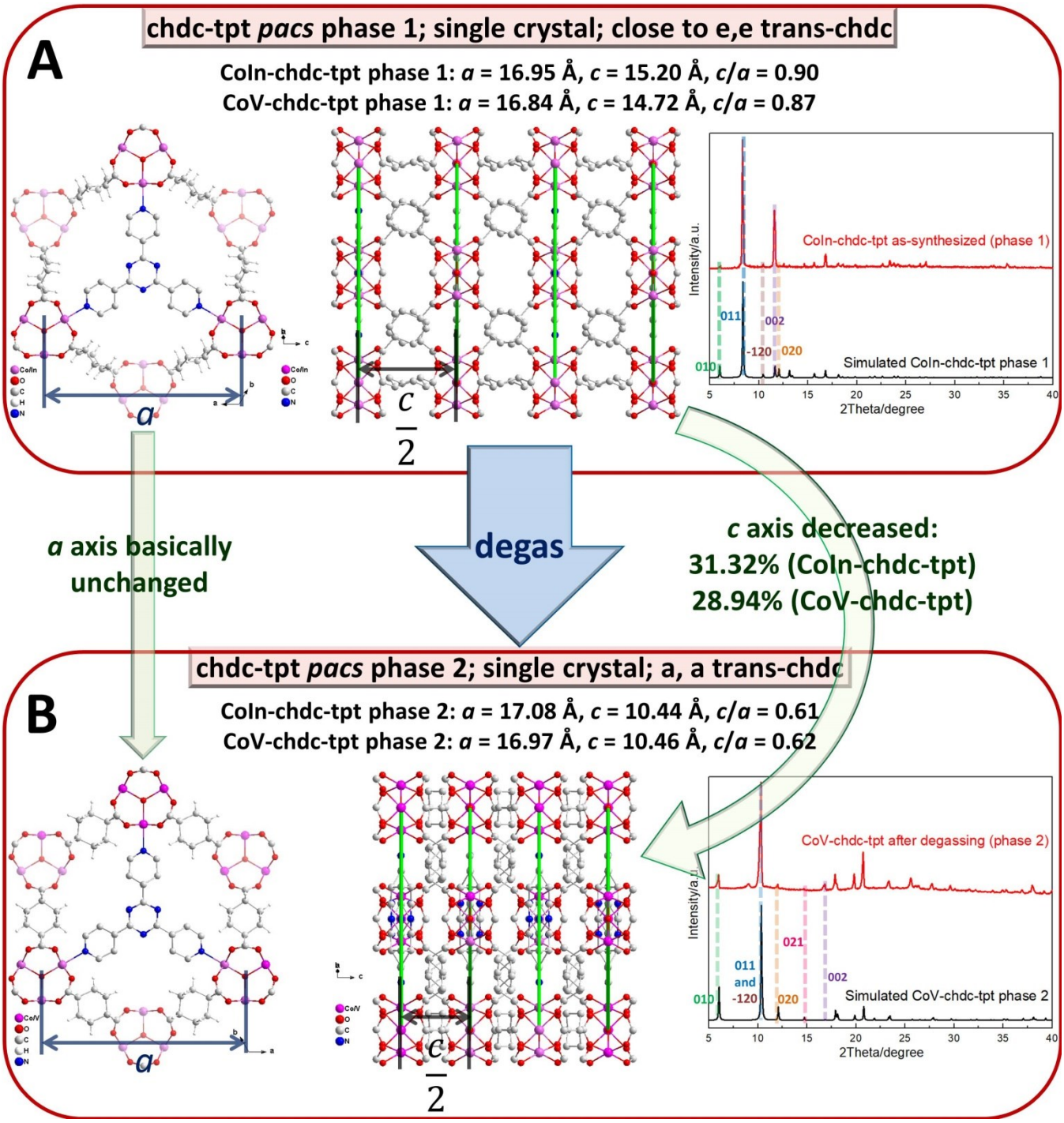

Figure 2. Comparing cell parameters, structures, and PXRD patterns between phase 1 (A) and phase 2 (B) of chdc-tpt *pacs*. The near-constancy of *a*/*b*-axis and shortening of the *c*-axis correlate with the rigidifying effect of tpt and the flexibility of chdc.

The near-constancy of the *a*/*b* axis and the large change in the *c* axis impact PXRD peaks in dramatically different ways depending on the peak indices. PXRD shows that the (010) peak ($l = 0$) has little shift (only 0.10° for CoIn) while the (011) peak ($l \neq 0$) undergoes large shift (2.12° for CoIn) from phase 1 to phase 2 (**Figure S12A**). Such phenomenon is unusual. Few porous materials are capable of retaining X-ray-quality single crystallinity after degassing and such large axial change (**Table S10**).[26-32, 46-65] Clearly, the simultaneous control of flexibility with L1 and rigidity with L2 plays an important role in maintaining single-crystallinity and porosity.

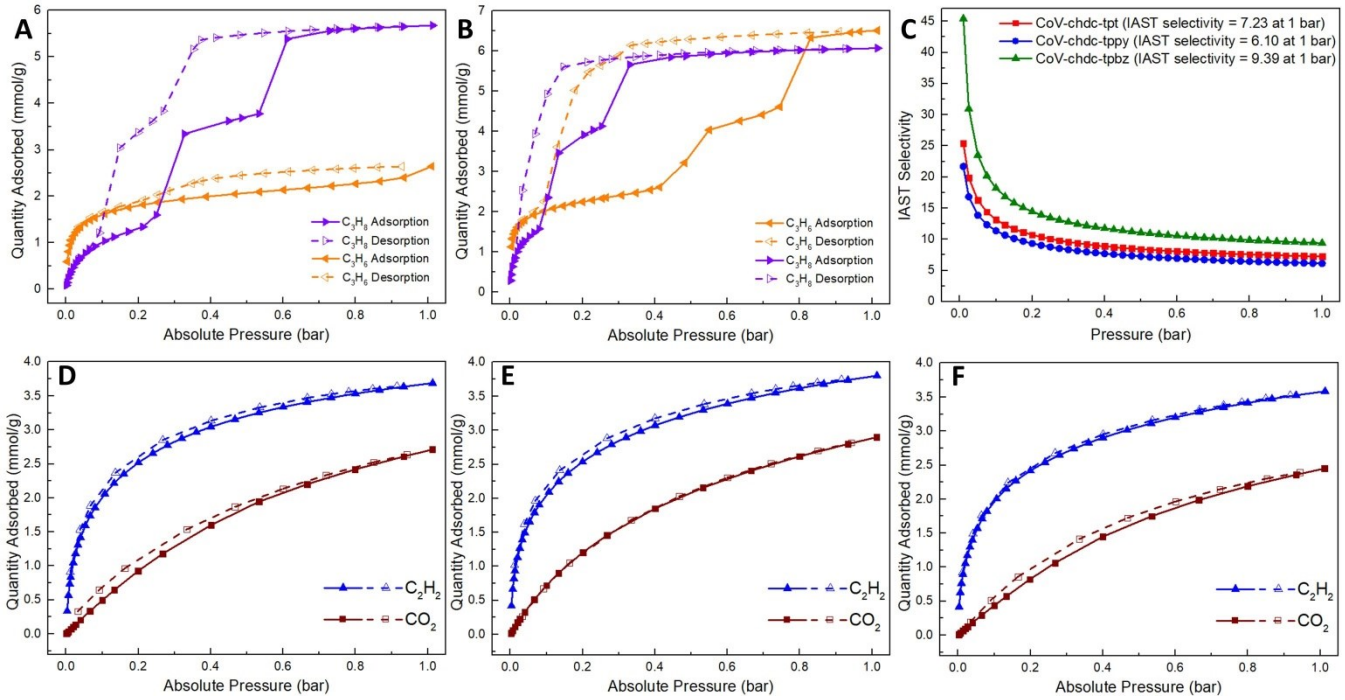

Figure 3. C_3H_6 and C_3H_8 isotherms of CoV-chdc-tpt at 298 K (A) and 273 K (B). C_2H_2/CO_2 IAST (50/50) selectivities of CoV-chdc *pacs* at 298 K (C). C_2H_2 and CO_2 isotherms of CoV-chdc-tpt (D), CoV-chdc-tppy (E), and CoV-chdc-tpbz (F) at 298K.

The large change in *c* axis can be understood from structural features. First, since trimers follow the ABAB stacking sequence, *c*-axis length is affected by two L1 ligands so that the length change in L1 is magnified in *c* axial change. Literature shows that the distances between two COO^- groups (based on C in COO^-) of chdc are about 5.85 and 4.89 Å in the e,e and a,a forms, respectively (**Figure S2**).[66-67] Our single crystal analysis shows that CPM-220 phase 1 is close to the e,e form (**Figure S5**), while phase 2 has the a,a form (**Figure S10**). Secondly, compared to other L1 ligands, the a,a form is exceptional because it is the first *pacs* example in which two COO^- planes are not coplanar, but have an offset of 3.18 Å in CoV-chdc-tpt phase 2. Such non-coplanarity is another reason for the short *c* axis. The greater the offset, the shorter the *c* axis (**Figure S20**). Note that this offset is different from other situations such as 2,6-ndc where two COO^- are not colinear, but are still coplanar (**Scheme 1**). The offset concept is more general than the e,e and a,a forms which are two extreme cases corresponding to start and end points of the phase transition between phase 1 and phase 2.

Thermal stability of CPM-220 with different metals (**Figure S11B**) and different L2 ligands (**Figure S11D**) were studied by TGA and all samples remained stable up to about 400 °C. Different compositions of CPM-220 phase 2 were used for gas sorption studies. PXRD shows no difference in diffraction patterns before and after sorption, suggesting all samples were stable after repeated adsorption-desorption cycles (**Figures S12**, **S15**, **S17**, **S18**). The Brunauer–Emmett–Teller (BET) surface area was determined by N_2 sorption at 77 K (**Figure S24**) and is 589 m^2/g for CoIn-chdc-tpt. For CoV-chdc compositions, it is 617 (tpt), 541 (tppy), and 545 (tpbz) m^2/g (**Table S6**). These numbers indicate highly porous nature of CPM-220 phase 2.

The adsorption/desorption isotherms for different gases at 298 K and 273 K show that CPM-220 exhibit normal gas sorption properties as well as unusual gate-opening effects depending on temperature and size of the probe molecule.[9, 64, 68-72] Overall, the trend is that lower temperature or larger gas molecules lead to lower pressure for gate opening. This can be understood by greater pore-filling and resulting greater steric interactions at lower temperature or with larger molecules.[5, 73-79] For CoV-chdc-tpt, the isotherms for CO_2, C_2H_2, C_2H_4, and C_2H_6 show type I at both temperatures except for C_2H_6 at 273 K which shows a steeper rise starting at about 0.9 bar (**Figure S28**). Unusual behaviors were observed for C_3H_6 and C_3H_8. While C_3H_6 shows a nearly type I isotherm at 298 K,[64, 70, 80-82] C_3H_8 shows a multi-step rise, as well as a hysteresis loop (**Figure 3A**).[70, 83] Yet, at 273 K, both C_3H_6 and C_3H_8 exhibit a multi-step adsorption (**Figure 3B**) with C_3H_6 showing a larger hysteresis loop, because the gate-opening pressure for C_3H_6 is higher than that of C_3H_8. PXRD confirms that the phase 2 structure is restored after the adsorption-desorption cycle (**Figure S15A**). The reproducibility of C_3H_6 and C_3H_8 isotherms at both 298 K and 273 K were confirmed by multiple cycles of measurements on the same samples as well as with different batches of samples performed (**Figure S29**).

The size and temperature dependent gate-opening behaviors by C_3H_6 and C_3H_8 have a large impact on the relative uptake for C_3H_6 and C_3H_8 for CoV-chdc-tpt. At 273 K and 1 bar, C_3H_6 and C_3H_8 uptakes are both high at 6.52 mmol/g and 6.08 mmol/g, respectively, because both gases can open the pore. Yet, at 298 K and 1 bar, the uptake for C_3H_6 is suppressed (no gate opening for C_3H_6) while C_3H_8 can still open the pore, leading to quite different C_3H_6 and C_3H_8 uptakes of 2.65 mmol/g and 5.68 mmol/g at 1 bar, respectively (**Table S6**).

CPM-220 has good C_2H_2/CO_2 selective adsorption property that can be tuned with L2 ligands. At 298 K and 1 bar, the C_2H_2 and CO_2 uptake are 3.69 and 2.71 mmol/g for CoV-chdc-tpt, 3.80 and 2.90 mmol/g for CoV-chdc-tppy, and 3.58 and 2.45 mmol/g for CoV-chdc-tpbz (**Figure 3D-F**, **Table S6**). The isotherms of C_2H_2 and CO_2 at 298 K were used to fit with the Dual-Site Langmuir-Freundlich (DSLF) model to calculate

the ideal adsorbed solution theory (IAST, 50/50) selectivities for CoV-chdc-tpt (7.23), CoV-chdc-tppy (6.10), and CoV-chdc-tpbz (9.39) (**Figure 3C, Table S8**). It is expected that the selectivity can be further improved by varying trimer compositions.

The modular synthesis also allows us to tune CPM-220 compositions to achieve excellent benzene/cyclohexane selective adsorption property. Both CoV-chdc-tppy and CoV-chdc-tpbz adsorb negligible amount of cyclohexane, but adsorb a large amount of benzene (**Figures S39-S56**), which is close to the molecular sieve effect (**Table S9**).

In conclusion, we have developed a series of multi-modular *pacs* materials (CPM-220) that have altered our understanding of the *pacs* platform as being a rigid type. The co-existence of flexibility and rigidity makes it possible to push down the pore size without losing porosity, and also results in unusual single-crystal to single-crystal transformation despite huge unit cell change (about 30%) under harsh conditions. The pore optimization achieved with CPM-220 has led to unusual sorption behaviors towards C_3H_6 and C_3H_8, promising C_2H_2/CO_2 separation performance, and highly selective benzene/cyclohexane separation property.

ASSOCIATED CONTENT

Supporting Information.
The Supporting Information is available free of charge at http://XXXXXX.
Experimental Procedures and compound characterization data (PDF).
CCDC 2192229, 2209904, 2255573, and 2257299 contain the supplementary crystallographic data for this paper. These data can be obtained free of charge via www.ccdc.cam.ac.uk/data_request/cif, or by emailing data_request@ccdc.cam.ac.uk, or by contacting The Cambridge Crystallographic Data Centre, 12 Union Road, Cambridge CB2 1EZ, U.K.; fax: +44 1223 336033.

AUTHOR INFORMATION

Corresponding Author

*pingyun.feng@ucr.edu, xianhui.bu@csulb.edu

Notes

The authors declare no competing financial interests.

ACKNOWLEDGMENT

We acknowledge the support of this work by the US Department of Energy, Office of Basic Energy Sciences, Materials Sciences and Engineering Division under Award No. DE-SC0010596 (P.F.). The single-crystal X-ray diffraction analysis was made possible by an NSF MRI grant (CHEM 2117040, X. B.).

REFERENCES

1. Ding, M.; Flaig, R. W.; Jiang, H.-L.; Yaghi, O. M., Carbon capture and conversion using metal–organic frameworks and MOF-based materials. *Chem. Soc. Rev.* **2019,** *48* (10), 2783-2828.
2. Tran, L. D.; Feldblyum, J. I.; Wong-Foy, A. G.; Matzger, A. J., Filling Pore Space in a Microporous Coordination Polymer to Improve Methane Storage Performance. *Langmuir* **2015,** *31* (7), 2211-2217.
3. Zhang, Z.; Yao, Z.-Z.; Xiang, S.; Chen, B., Perspective of microporous metal–organic frameworks for CO2 capture and separation. *Energy Environ. Sci.* **2014,** *7* (9), 2868-2899.
4. Bao, Z.; Chang, G.; Xing, H.; Krishna, R.; Ren, Q.; Chen, B., Potential of microporous metal–organic frameworks for separation of hydrocarbon mixtures. *Energy Environ. Sci.* **2016,** *9* (12), 3612-3641.
5. Wang, H.; Dong, X.; Colombo, V.; Wang, Q.; Liu, Y.; Liu, W.; Wang, X.-L.; Huang, X.-Y.; Proserpio, D. M.; Sironi, A.; Han, Y.; Li, J., Tailor-Made Microporous Metal–Organic Frameworks for the Full Separation of Propane from Propylene Through Selective Size Exclusion. *Adv. Mater.* **2018,** *30* (49), 1805088.
6. Xue, D.-X.; Cadiau, A.; Weseliński, Ł. J.; Jiang, H.; Bhatt, P. M.; Shkurenko, A.; Wojtas, L.; Zhijie, C.; Belmabkhout, Y.; Adil, K.; Eddaoudi, M., Topology meets MOF chemistry for pore-aperture fine tuning: ftw-MOF platform for energy-efficient separations via adsorption kinetics or molecular sieving. *ChemComm* **2018,** *54* (49), 6404-6407.
7. Liang, B.; Zhang, X.; Xie, Y.; Lin, R.-B.; Krishna, R.; Cui, H.; Li, Z.; Shi, Y.; Wu, H.; Zhou, W.; Chen, B., An Ultramicroporous Metal–Organic Framework for High Sieving Separation of Propylene from Propane. *J. Am. Chem. Soc.* **2020,** *142* (41), 17795-17801.
8. Yu, L.; Han, X.; Wang, H.; Ullah, S.; Xia, Q.; Li, W.; Li, J.; da Silva, I.; Manuel, P.; Rudić, S.; Cheng, Y.; Yang, S.; Thonhauser, T.; Li, J., Pore Distortion in a Metal–Organic Framework for Regulated Separation of Propane and Propylene. *J. Am. Chem. Soc.* **2021,** *143* (46), 19300-19305.
9. Li, H.; Li, L.; Lin, R.-B.; Zhou, W.; Zhang, Z.; Xiang, S.; Chen, B., Porous metal-organic frameworks for gas storage and separation: Status and challenges. *EnergyChem* **2019,** *1* (1), 100006.
10. Zhai, Q.-G.; Bu, X.; Zhao, X.; Li, D.-S.; Feng, P., Pore Space Partition in Metal–Organic Frameworks. *Acc. Chem. Res.* **2017,** *50* (2), 407-417.
11. Hong, A. N.; Yang, H.; Bu, X.; Feng, P., Pore space partition of metal-organic frameworks for gas storage and separation. *EnergyChem* **2022,** *4* (4), 100080.
12. Zheng, S.-T.; Zhao, X.; Lau, S.; Fuhr, A.; Feng, P.; Bu, X., Entrapment of Metal Clusters in Metal–Organic Framework Channels by Extended Hooks Anchored at Open Metal Sites. *J. Am. Chem. Soc.* **2013,** *135* (28), 10270-10273.
13. Zhao, X.; Bu, X.; Zhai, Q.-G.; Tran, H.; Feng, P., Pore Space Partition by Symmetry-Matching Regulated Ligand Insertion and Dramatic Tuning on Carbon Dioxide Uptake. *J. Am. Chem. Soc.* **2015,** *137* (4), 1396-1399.
14. Zhai, Q.-G.; Bu, X.; Mao, C.; Zhao, X.; Daemen, L.; Cheng, Y.; Ramirez-Cuesta, A. J.; Feng, P., An ultra-tunable platform for molecular engineering of high-performance crystalline porous materials. *Nat. Commun.* **2016,** *7*, 13645.
15. Zhao, X.; Bu, X.; Nguyen, E. T.; Zhai, Q.-G.; Mao, C.; Feng, P., Multivariable Modular Design of Pore Space Partition. *J. Am. Chem. Soc.* **2016,** *138* (46), 15102-15105.
16. Wang, Y.; Zhao, X.; Yang, H.; Bu, X.; Wang, Y.; Jia, X.; Li, J.; Feng, P., A Tale of Two Trimers from Two Different Worlds: A COF-Inspired Synthetic Strategy for Pore-Space Partitioning of MOFs. *Angew. Chem. Int. Ed.* **2019,** *58* (19), 6316-6320.
17. Wang, Y.; Jia, X.; Yang, H.; Wang, Y.; Chen, X.; Hong, A. N.; Li, J.; Bu, X.; Feng, P., A Strategy for Constructing Pore-Space-Partitioned MOFs with High Uptake Capacity for C2 Hydrocarbons and CO2. *Angew. Chem.* **2020,** *132* (43), 19189-19192.
18. Yang, H.; Wang, Y.; Krishna, R.; Jia, X.; Wang, Y.; Hong, A. N.; Dang, C.; Castillo, H. E.; Bu, X.; Feng, P., Pore-Space-Partition-Enabled Exceptional Ethane Uptake and Ethane-Selective Ethane–Ethylene Separation. *J. Am. Chem. Soc.* **2020,** *142* (5), 2222-2227.
19. Hong, A. N.; Yang, H.; Li, T.; Wang, Y.; Wang, Y.; Jia, X.; Zhou, A.; Kusumoputro, E.; Li, J.; Bu, X.; Feng, P., Pore-Space Partition and Optimization for Propane-Selective High-Performance Propane/Propylene Separation. *ACS Appl. Mater. Interfaces* **2021,** *13* (44), 52160-52166.
20. Yang, H.; Peng, F.; Hong, A. N.; Wang, Y.; Bu, X.; Feng, P., Ultrastable High-Connected Chromium Metal–Organic Frameworks. *J. Am. Chem. Soc.* **2021,** *143* (36), 14470-14474.
21. Hong, A. N.; Kusumoputro, E.; Wang, Y.; Yang, H.; Chen, Y.; Bu, X.; Feng, P., Simultaneous Control of Pore-Space Partition and Charge Distribution in Multi-Modular Metal–Organic Frameworks. *Angew. Chem. Int. Ed.* **2022,** *61* (13), e202116064.

22. Yang, H.; Chen, Y.; Dang, C.; Hong, A. N.; Feng, P.; Bu, X., Optimization of Pore-Space-Partitioned Metal–Organic Frameworks Using the Bioisosteric Concept. *J. Am. Chem. Soc.* **2022,** *144* (44), 20221-20226.
23. Xiao, Y.; Hong, A. N.; Chen, Y.; Yang, H.; Wang, Y.; Bu, X.; Feng, P., Developing Water-Stable Pore-Partitioned Metal-Organic Frameworks with Multi-Level Symmetry for High-Performance Sorption Applications. *Small* **2023,** *19* (5), 2205119.
24. Xiao, Y.; Chen, Y.; Hong, A. N.; Bu, X.; Feng, P., Solvent-free Synthesis of Multi-Module Pore-Space-Partitioned Metal-Organic Frameworks for Gas Separation. *Angew. Chem. Int. Ed.* **2023,** *62* (14), e202300721.
25. Wei, Y.-S.; Zhang, M.; Liao, P.-Q.; Lin, R.-B.; Li, T.-Y.; Shao, G.; Zhang, J.-P.; Chen, X.-M., Coordination templated [2+2+2] cyclotrimerization in a porous coordination framework. *Nat. Commun.* **2015,** *6* (1), 8348.
26. Zhang, Y.; Zhang, X.; Lyu, J.; Otake, K.-i.; Wang, X.; Redfern, L. R.; Malliakas, C. D.; Li, Z.; Islamoglu, T.; Wang, B.; Farha, O. K., A Flexible Metal–Organic Framework with 4-Connected Zr6 Nodes. *J. Am. Chem. Soc.* **2018,** *140* (36), 11179-11183.
27. Yuan, S.; Zou, L.; Li, H.; Chen, Y.-P.; Qin, J.; Zhang, Q.; Lu, W.; Hall, M. B.; Zhou, H.-C., Flexible Zirconium Metal-Organic Frameworks as Bioinspired Switchable Catalysts. *Angew. Chem. Int. Ed.* **2016,** *55* (36), 10776-10780.
28. Demessence, A.; Long, J. R., Selective Gas Adsorption in the Flexible Metal–Organic Frameworks Cu(BDTri)L (L=DMF, DEF). *Chem. Eur. J.* **2010,** *16* (20), 5902-5908.
29. Zhang, Y.; Zhang, X.; Chen, Z.; Otake, K.-i.; Peterson, G. W.; Chen, Y.; Wang, X.; Redfern, L. R.; Goswami, S.; Li, P.; Islamoglu, T.; Wang, B.; Farha, O. K., A Flexible Interpenetrated Zirconium-Based Metal–Organic Framework with High Affinity toward Ammonia. *ChemSusChem* **2020,** *13* (7), 1710-1714.
30. Yang, F.; Xu, G.; Dou, Y.; Wang, B.; Zhang, H.; Wu, H.; Zhou, W.; Li, J.-R.; Chen, B., A flexible metal–organic framework with a high density of sulfonic acid sites for proton conduction. *Nat. Energy.* **2017,** *2* (11), 877-883.
31. Dong, Q.; Zhang, X.; Liu, S.; Lin, R.-B.; Guo, Y.; Ma, Y.; Yonezu, A.; Krishna, R.; Liu, G.; Duan, J.; Matsuda, R.; Jin, W.; Chen, B., Tuning Gate-Opening of a Flexible Metal–Organic Framework for Ternary Gas Sieving Separation. *Angew. Chem. Int. Ed.* **2020,** *59* (50), 22756-22762.
32. Kim, J. Y.; Park, J.; Ha, J.; Jung, M.; Wallacher, D.; Franz, A.; Balderas-Xicohténcatl, R.; Hirscher, M.; Kang, S. G.; Park, J. T.; Oh, I. H.; Moon, H. R.; Oh, H., Specific Isotope-Responsive Breathing Transition in Flexible Metal–Organic Frameworks. *J. Am. Chem. Soc.* **2020,** *142* (31), 13278-13282.
33. Surblé, S.; Serre, C.; Mellot-Draznieks, C.; Millange, F.; Férey, G., A new isoreticular class of metal-organic-frameworks with the MIL-88 topology. *ChemComm* **2006,** (3), 284-286.
34. Morris, R. E.; Brammer, L., Coordination change, lability and hemilability in metal–organic frameworks. *Chem. Soc. Rev.* **2017,** *46* (17), 5444-5462.
35. Elsaidi, S. K.; Mohamed, M. H.; Banerjee, D.; Thallapally, P. K., Flexibility in Metal–Organic Frameworks: A fundamental understanding. *Coord. Chem. Rev.* **2018,** *358*, 125-152.
36. Parent, L. R.; Pham, C. H.; Patterson, J. P.; Denny, M. S., Jr.; Cohen, S. M.; Gianneschi, N. C.; Paesani, F., Pore Breathing of Metal–Organic Frameworks by Environmental Transmission Electron Microscopy. *J. Am. Chem. Soc.* **2017,** *139* (40), 13973-13976.
37. Cui, H.; Ye, Y.; Liu, T.; Alothman, Z. A.; Alduhaish, O.; Lin, R.-B.; Chen, B., Isoreticular Microporous Metal–Organic Frameworks for Carbon Dioxide Capture. *Inorg. Chem.* **2020,** *59* (23), 17143-17148.
38. Dutta, A.; Pan, Y.; Liu, J.-Q.; Kumar, A., Multicomponent isoreticular metal-organic frameworks: Principles, current status and challenges. *Coord. Chem. Rev.* **2021,** *445*, 214074.
39. Eddaoudi, M.; Kim, J.; Rosi, N.; Vodak, D.; Wachter, J.; O'Keeffe, M.; Yaghi, O. M., Systematic Design of Pore Size and Functionality in Isoreticular MOFs and Their Application in Methane Storage. *Science* **2002,** *295* (5554), 469-472.
40. Lin, R.-B.; Zhang, Z.; Chen, B., Achieving High Performance Metal–Organic Framework Materials through Pore Engineering. *Acc. Chem. Res.* **2021,** *54* (17), 3362-3376.
41. Bueken, B.; Vermoortele, F.; Vanpoucke, D. E. P.; Reinsch, H.; Tsou, C.-C.; Valvekens, P.; De Baerdemaeker, T.; Ameloot, R.; Kirschhock, C. E. A.; Van Speybroeck, V.; Mayer, J. M.; De Vos, D., A Flexible Photoactive Titanium Metal–Organic Framework Based on a [TiIV3(μ3-O)(O)2(COO)6] Cluster. *Angew. Chem. Int. Ed.* **2015,** *54* (47), 13912-13917.
42. Bueken, B.; Vermoortele, F.; Cliffe, M. J.; Wharmby, M. T.; Foucher, D.; Wieme, J.; Vanduyfhuys, L.; Martineau, C.; Stock, N.; Taulelle, F.; Van Speybroeck, V.; Goodwin, A. L.; De Vos, D., A Breathing Zirconium Metal–Organic Framework with Reversible Loss of Crystallinity by Correlated Nanodomain Formation. *Chem. Eur. J.* **2016,** *22* (10), 3264-3267.
43. Niekiel, F.; Lannoeye, J.; Reinsch, H.; Munn, A. S.; Heerwig, A.; Zizak, I.; Kaskel, S.; Walton, R. I.; de Vos, D.; Llewellyn, P.; Lieb, A.; Maurin, G.; Stock, N., Conformation-Controlled Sorption Properties and Breathing of the Aliphatic Al-MOF [Al(OH)(CDC)]. *Inorg. Chem.* **2014,** *53* (9), 4610-4620.
44. Zhang, M.-D.; Di, C.-M.; Qin, L.; Yao, X.-Q.; Li, Y.-Z.; Guo, Z.-J.; Zheng, H.-G., Diverse Structures of Metal–Organic Frameworks Based on a New Star-Like Tri(4-pyridylphenyl)amine Ligand. *Cryst. Growth Des.* **2012,** *12* (8), 3957-3963.
45. Snyder, B. E. R.; Turkiewicz, A. B.; Furukawa, H.; Paley, M. V.; Velasquez, E. O.; Dods, M. N.; Long, J. R., A ligand insertion mechanism for cooperative NH3 capture in metal–organic frameworks. *Nature* **2023,** *613* (7943), 287-291.
46. Maji, T. K.; Mostafa, G.; Matsuda, R.; Kitagawa, S., Guest-Induced Asymmetry in a Metal−Organic Porous Solid with Reversible Single-Crystal-to-Single-Crystal Structural Transformation. *J. Am. Chem. Soc.* **2005,** *127* (49), 17152-17153.
47. Park, H. J.; Suh, M. P., Mixed-Ligand Metal–Organic Frameworks with Large Pores: Gas Sorption Properties and Single-Crystal-to-Single-Crystal Transformation on Guest Exchange. *Chem. Eur. J.* **2008,** *14* (29), 8812-8821.
48. Gustafsson, M.; Su, J.; Yue, H.; Yao, Q.; Zou, X., A Family of Flexible Lanthanide Bipyridinedicarboxylate Metal–Organic Frameworks Showing Reversible Single-Crystal to Single-Crystal Transformations. *Cryst. Growth Des.* **2012,** *12* (6), 3243-3249.
49. Kyprianidou, E. J.; Papaefstathiou, G. S.; Manos, M. J.; Tasiopoulos, A. J., A flexible Cd2+ metal organic framework with a unique (3,3,6)-connected topology, unprecedented secondary building units and single crystal to single crystal solvent exchange properties. *CrystEngComm* **2012,** *14* (24), 8368-8373.
50. Lee, J. H.; Kim, T. K.; Suh, M. P.; Moon, H. R., Solvent-induced single-crystal to single-crystal transformation of a Zn4O-containing doubly interpenetrated metal–organic framework with a pcu net. *CrystEngComm* **2015,** *17* (46), 8807-8811.
51. Mason, J. A.; Oktawiec, J.; Taylor, M. K.; Hudson, M. R.; Rodriguez, J.; Bachman, J. E.; Gonzalez, M. I.; Cervellino, A.; Guagliardi, A.; Brown, C. M.; Llewellyn, P. L.; Masciocchi, N.; Long, J. R., Methane storage in flexible metal–organic frameworks with intrinsic thermal management. *Nature* **2015,** *527* (7578), 357-361.
52. Wang, C.; Li, L.; Bell, J. G.; Lv, X.; Tang, S.; Zhao, X.; Thomas, K. M., Hysteretic Gas and Vapor Sorption in Flexible Interpenetrated Lanthanide-Based Metal–Organic Frameworks with Coordinated Molecular Gating via Reversible Single-Crystal-to-Single-Crystal Transformation for Enhanced Selectivity. *Chem. Mater.* **2015,** *27* (5), 1502-1516.
53. Agarwal, R. A.; Mukherjee, S., Two-dimensional flexible Ni(II)-based porous coordination polymer showing single-crystal to single-crystal transformation, selective gas adsorption and catalytic properties. *Polyhedron* **2016,** *105*, 228-237.
54. Ganguly, S.; Mukherjee, S.; Dastidar, P., Single-Crystal-to-Single-Crystal Breathing and Guest Exchange in CoII Metal–Organic Frameworks. *Cryst. Growth Des.* **2016,** *16* (9), 5247-5259.
55. Spirkl, S.; Grzywa, M.; Reschke, S.; Fischer, J. K. H.; Sippel, P.; Demeshko, S.; Krug von Nidda, H.-A.; Volkmer, D., Single-Crystal to Single-Crystal Transformation of a Nonporous Fe(II) Metal–

Organic Framework into a Porous Metal–Organic Framework via a Solid-State Reaction. *Inorg. Chem.* **2017,** *56* (20), 12337-12347.
56. Wang, L.; He, W.-W.; Yao, Z.-Q.; Hu, T.-L., A Flexible Porous MOF Exhibiting Reversible Breathing Behavior through Single-Crystal to Single-Crystal Transformation. *ChemistrySelect* **2017,** *2* (1), 283-287.
57. Yang, X.-Y.; Yuan, S.; Qin, J.-S.; Lollar, C.; Alsalme, A.; Zhou, H.-C., A flexible thioether-based MOF as a crystalline sponge for structural characterization of liquid organic molecules. *Mater. Chem. Front.* **2017,** *1* (9), 1764-1767.
58. Ye, Z.-M.; He, C.-T.; Xu, Y.-T.; Krishna, R.; Xie, Y.; Zhou, D.-D.; Zhou, H.-L.; Zhang, J.-P.; Chen, X.-M., A New Isomeric Porous Coordination Framework Showing Single-Crystal to Single-Crystal Structural Transformation and Preferential Adsorption of 1,3-Butadiene from C4 Hydrocarbons. *Cryst. Growth Des.* **2017,** *17* (4), 2166-2171.
59. Dong, X.-Y.; Huang, H.-L.; Wang, J.-Y.; Li, H.-Y.; Zang, S.-Q., A Flexible Fluorescent SCC-MOF for Switchable Molecule Identification and Temperature Display. *Chem. Mater.* **2018,** *30* (6), 2160-2167.
60. Shivanna, M.; Yang, Q.-Y.; Bajpai, A.; Patyk-Kazmierczak, E.; Zaworotko, M. J., A dynamic and multi-responsive porous flexible metal–organic material. *Nat. Commun.* **2018,** *9* (1), 3080.
61. Spirkl, S.; Grzywa, M.; Volkmer, D., Synthesis and characterization of a flexible metal organic framework generated from MnIII and the 4,4′-bipyrazolate-ligand. *Dalton Trans.* **2018,** *47* (26), 8779-8786.
62. Hanna, S. L.; Zhang, X.; Otake, K.-i.; Drout, R. J.; Li, P.; Islamoglu, T.; Farha, O. K., Guest-Dependent Single-Crystal-to-Single-Crystal Phase Transitions in a Two-Dimensional Uranyl-Based Metal–Organic Framework. *Cryst. Growth Des.* **2019,** *19* (1), 506-512.
63. Hazra, A.; van Heerden, D. P.; Sanyal, S.; Lama, P.; Esterhuysen, C.; Barbour, L. J., CO2-induced single-crystal to single-crystal transformations of an interpenetrated flexible MOF explained by in situ crystallographic analysis and molecular modeling. *Chem. Sci.* **2019,** *10* (43), 10018-10024.
64. Bonneau, M.; Sugimoto, K.; Otake, K.-i.; Tsuji, Y.; Shimanaka, N.; Lavenn, C.; Kitagawa, S., Guest-selective gate-opening by pore engineering of two-dimensional Kagomè lattice porous coordination polymers. *Nat. sci.* **2021,** *1* (2), e10020.
65. Peralta, R. A.; Huxley, M. T.; Young, R. J.; Linder-Patton, O. M.; Evans, J. D.; Doonan, C. J.; Sumby, C. J., MOF matrix isolation: cooperative conformational mobility enables reliable single crystal transformations. *Faraday Discuss.* **2021,** *225* (0), 84-99.
66. Thuéry, P.; Harrowfield, J., Structural Consequences of 1,4-Cyclohexanedicarboxylate Cis/Trans Isomerism in Uranyl Ion Complexes: From Molecular Species to 2D and 3D Entangled Nets. *Inorg. Chem.* **2017,** *56* (21), 13464-13481.
67. Demakov, P. A.; Sapchenko, S. A.; Samsonenko, D. G.; Dybtsev, D. N.; Fedin, V. P., Coordination polymers based on zinc(ii) and manganese(ii) with 1,4-cyclohexanedicarboxylic acid. *Russ. Chem. Bull.* **2018,** *67* (3), 490-496.
68. Hamon, L.; Llewellyn, P. L.; Devic, T.; Ghoufi, A.; Clet, G.; Guillerm, V.; Pirngruber, G. D.; Maurin, G.; Serre, C.; Driver, G.; van Beek, W.; Jolimaître, E.; Vimont, A.; Daturi, M.; Férey, G., Co-adsorption and Separation of CO2−CH4 Mixtures in the Highly Flexible MIL-53(Cr) MOF. *J. Am. Chem. Soc.* **2009,** *131* (47), 17490-17499.
69. Nijem, N.; Wu, H.; Canepa, P.; Marti, A.; Balkus, K. J.; Thonhauser, T.; Li, J.; Chabal, Y. J., Tuning the Gate Opening Pressure of Metal–Organic Frameworks (MOFs) for the Selective Separation of Hydrocarbons. *J. Am. Chem. Soc.* **2012,** *134* (37), 15201-15204.
70. Quartapelle Procopio, E.; Fukushima, T.; Barea, E.; Navarro, J. A. R.; Horike, S.; Kitagawa, S., A Soft Copper(II) Porous Coordination Polymer with Unprecedented Aqua Bridge and Selective Adsorption Properties. *Chem. Eur. J.* **2012,** *18* (41), 13117-13125.
71. Krause, S.; Hosono, N.; Kitagawa, S., Chemistry of Soft Porous Crystals: Structural Dynamics and Gas Adsorption Properties. *Angew. Chem. Int. Ed.* **2020,** *59* (36), 15325-15341.
72. Wang, Z.; Cohen, S. M., Modulating Metal−Organic Frameworks To Breathe: A Postsynthetic Covalent Modification Approach. *J. Am. Chem. Soc.* **2009,** *131* (46), 16675-16677.
73. Yang, Y.; Li, L.; Lin, R.-B.; Ye, Y.; Yao, Z.; Yang, L.; Xiang, F.; Chen, S.; Zhang, Z.; Xiang, S.; Chen, B., Ethylene/ethane separation in a stable hydrogen-bonded organic framework through a gating mechanism. *Nat. Chem.* **2021,** *13* (10), 933-939.
74. van den Bergh, J.; Gücüyener, C.; Pidko, E. A.; Hensen, E. J. M.; Gascon, J.; Kapteijn, F., Understanding the Anomalous Alkane Selectivity of ZIF-7 in the Separation of Light Alkane/Alkene Mixtures. *Chem. Eur. J.* **2011,** *17* (32), 8832-8840.
75. Selzer, C.; Werner, A.; Kaskel, S., Selective Adsorption of Propene over Propane on Hierarchical Zeolite ZSM-58. *Ind. Eng. Chem. Res.* **2018,** *57* (19), 6609-6617.
76. Liu, Y.; Wu, Y.; Liang, W.; Peng, J.; Li, Z.; Wang, H.; Janik, M. J.; Xiao, J., Bimetallic ions regulate pore size and chemistry of zeolites for selective adsorption of ethylene from ethane. *Chem. Eng. Sci.* **2020,** *220*, 115636.
77. Lyndon, R.; You, W.; Ma, Y.; Bacsa, J.; Gong, Y.; Stangland, E. E.; Walton, K. S.; Sholl, D. S.; Lively, R. P., Tuning the Structures of Metal–Organic Frameworks via a Mixed-Linker Strategy for Ethylene/Ethane Kinetic Separation. *Chem. Mater.* **2020,** *32* (9), 3715-3722.
78. Wang, X.; Zhang, P.; Zhang, Z.; Yang, L.; Ding, Q.; Cui, X.; Wang, J.; Xing, H., Efficient Separation of Propene and Propane Using Anion-Pillared Metal–Organic Frameworks. *Ind. Eng. Chem. Res.* **2020,** *59* (8), 3531-3537.
79. Zhang, X.-W.; Zhou, D.-D.; Zhang, J.-P., Tuning the gating energy barrier of metal-organic framework for molecular sieving. *Chem* **2021,** *7* (4), 1006-1019.
80. Donohue, M. D.; Aranovich, G. L., Classification of Gibbs adsorption isotherms. *Adv. Colloid Interface Sci.* **1998,** *76-77*, 137-152.
81. Kumar, K. V.; Gadipelli, S.; Wood, B.; Ramisetty, K. A.; Stewart, A. A.; Howard, C. A.; Brett, D. J. L.; Rodriguez-Reinoso, F., Characterization of the adsorption site energies and heterogeneous surfaces of porous materials. *J. Mater. Chem. A* **2019,** *7* (17), 10104-10137.
82. Rieth, A. J.; Dincă, M., Controlled Gas Uptake in Metal–Organic Frameworks with Record Ammonia Sorption. *J. Am. Chem. Soc.* **2018,** *140* (9), 3461-3466.
83. Fernandez, C. A.; Thallapally, P. K.; McGrail, B. P., Insights into the Temperature-Dependent “Breathing” of a Flexible Fluorinated Metal–Organic Framework. *ChemPhysChem* **2012,** *13* (14), 3275-3281.

Insert Table of Contents artwork here